European Journal of Medicinal Chemistry 48 (2012) 330–337

Contents lists available at SciVerse ScienceDirect

European Journal of Medicinal Chemistry

journal homepage: http://www.elsevier.com/locate/ejmech

Original article

Multifunctional gold nanorod theragnostics probed by multi-photon imaging

Brittany Book Newell, Yuling Wang, Joseph Irudayaraj*

Bindley Bioscience and Birck Nanotechnology Center, Purdue University, 225 S. University Street, West Lafayette, IN 47907, USA

ARTICLE INFO

Article history:
Received 13 March 2011
Received in revised form
21 December 2011
Accepted 23 December 2011
Available online 29 December 2011

Keywords:
Gold nanorods
Folic acid
Doxorubicin
Targeted drug delivery
Theragnostics
Multi-photon imaging

ABSTRACT

This study exhibits the fabrication of target-specific Gold nanorods (GNRs) coupled with an anti-tumorigenic apoptotic drug and provides tracking of the labeled particles as they migrate through cells and release their drug-load to targeted cancer cells. We utilize the photoluminescence property of GNRs and their ability to be conjugated with multiple agents to transform facile rods to a targeted drug delivery vehicle. GNRs of aspect ratio 2.8 were conjugated with a targeting ligand, folic acid and an anthracycline drug, Doxorubicin. The multifunctional nanorods were then used to target folate receptor expressing cancers cells for the delivery of a concentration dependent dosage of Doxorubicin (DOX). By utilizing the photoluminescence of GNRs and the innate fluorescence of DOX, multi-photon fluorescence lifetime imaging was utilized to monitor the uptake of functionalized nanorods, the release of the drug and its localization in living cells. We show that these nano-vehicles successfully targeted cancer cells over expressing folate receptors and showed low toxicity to control cell lines. Release of DOX was observed in the cytoplasmic region and after 16 h was found to be redistributed in the nucleus resulting in cell death. Our theragnostic approach demonstrates the fabrication of multifunctional GNRs for targeted drug delivery and monitoring of the drug and the vehicle by multi-photon microscopy using fluorescence intensity and lifetime imaging.

1. Introduction

The photophysics of the photoluminescence of noble metals can be explained briefly in three stages with the first being the construction of "electron holes" created by the excitation of valence electrons and their migration from the d-band to the sp-band. Following this process, the electrons and holes scatter resulting in the release of energy to the phonon lattice. The final step in the process is the recombination of the electron holes which causes a release of detectable photons [1]. The photoluminescence of noble metals can be probed using single or multi-photon laser excitation [2]. The multi-photon method facilitates deeper probing, enabling imaging of animal models.

In this article, we present a theragnostic approach of synthesizing and functionalizing gold nanorods (GNRs) with a cancer targeting antibody to target specific cancer cells and deliver an apoptotic drug while monitoring the drug distribution and localization of the photoluminescent delivery vehicle by multi-photon excitation. Gold nanorods have previously been constructed of various aspect ratios using several chemical synthesis methodologies including reduction by citrate [3], "Brust" synthesis [4] and, seed-mediated growth [5]. In our design, gold nanorods were constructed via a seed-mediated growth approach and stabilized with cetyltrimethylammonium bromide (CTAB) and 11-mercaptoundecanoic acid (MUA). The amino groups from this surface modification were used to functionalize the rods with targeting and therapeutic agents using covalent and electrostatic linkages.

Various types of cancers over express the folate receptors [6] because folic acid (FA) plays an active role in the synthesis and replication of DNA as well as in the prevention of DNA damage [7]. Since cancer cells are rapidly dividing, DNA replication must occur more frequently, resulting in an increased need for folic acid. Doxorubicin (DOX), a commonly used cell death inducing cancer therapeutic drug was used as the drug of choice to demonstrate the multifunctional attribute of gold nanorod based theragnostics. Folic acid was attached to gold nanorods using cystamine and DOX was attached through electrostatic binding. These nano-vehicles were then incubated with adherent KB cells. KB cells are cancer cells recovered from the nasopharynx which over express the folate receptor [6].

Doxorubicin, an anthracycline antibiotic and was originally discovered from the *Streptomyces peucetius* bacterium in the 1950s [8]. It is commonly used in cancer treatment either alone or in

* Corresponding author. Tel.: +1 765 494 0388; fax: +1 765 496 1115.
E-mail address: josephi@purdue.edu (J. Irudayaraj).

0223-5234/$ – see front matter © 2011 Elsevier Masson SAS. All rights reserved.
doi:10.1016/j.ejmech.2011.12.036

conjunction with other therapies. Doxorubicin induces cell death via intercalation of DNA and inhibition of the formation of macromolecules required for successful DNA repair and replication [8,9]. Doxorubicin inhibits an enzyme called topoisomerase II [9,10], which is responsible for the unwinding of DNA for transcription and DNA double-stranded breaks [8,11]. After the enzyme has broken the DNA for transcription, DOX locks it in this state, which prevents replication. Doxorubicin also exhibits high fluorescence (excitation ~470 nm and emission ~550–650 nm) and hence can be easily monitored by confocal microscopy.

Our study demonstrates the ability to load gold nanorods with a targeting molecule and a drug and to monitor distribution of the drug and delivery vehicle, within a living cancer cell. These goals can be accomplished using the photophysics of fluorescence. In our experiments, when DOX is bound to gold nanorods, the fluorescence of the drug is quenched until the drug is released from the nano-carrier. Release is triggered due to the cleavage of the electrostatic bonds mediated by changes in the intracellular pH. By time course experiments and multi-photon excitation we monitored cellular autofluorescence, GNR photoluminescence, and fluorescence of DOX to document the targeting, monitor the release, and assess the drug's effects on cancer cells [12].

2. Chemistry and pharmacology

GNRs were first modified by 11-mercaptoundecanoic acid (MUA) to obtain carboxyl-functionalized GNRs according to the method previously reported by our group and is depicted in Fig. 2C [13]. Briefly, 0.5 mL of 20 mM ethanol solution of MUA was added into 5 mL of the GNR solution and stirred at a moderate speed for 24 h under room temperature. The nanorods were then collected by centrifugation at 7000 rpm for 15 min and resuspended in a 0.005 M CTAB solution. In the next step GNRs were functionalized by an amino group according to the method previously reported by our group [14]. Here, 0.1 mL of 30 mM aqueous solution of cystamine was added into 1 mL of GNR solution and sonicated for 3 h at 50 °C. The resulting GNRs were then collected by centrifuging twice at 7000 rpm for 15 min to remove excess cystamine and CTAB and then resuspended in a 0.005 M CTAB solution. Then, to 1 mL of the activated GNRs, 200 μL of activated folic acid (in 3 mg/mL of folic acid, 500 μL of 0.4 M EDC and 500 μL of 0.1 M NHS solution was added and sonicated for 25 min at 4 °C) was added and sonicated at room temperature for 1 h. The resulting procedure allowed for the attachment of FA to the amino group through the EDC/NHS chemistry. The resulting GNRs were collected by centrifugation at 7000 rpm for 15 min and resuspended in PBS buffer (pH 7.4) containing 0.005 M CTAB to maintain monodispersity. Then 20 μL of 2.5 mg/mL Doxorubicin (DOX), the anti-tumorigenic drug was added into the resulting GNRs to facilitate its binding to the COOH groups from MUA through electrostatic binding between the drug (DOS is cationic) and the GNRs. After 3 h, the GNRs were centrifuged at 7000 rpm for 15 min to remove the free DOX and CTAB and then resuspended in PBS buffer for cancer cell targeting experiments.

3. Results and discussion

3.1. Characterization of GNRs by TEM image and UV–Vis absorption spectroscopy

The TEM image (Fig. 1) of the prepared GNRs, indicated that the GNRs are uniform in shape with an average length and aspect ratio of about 50 nm and 2.8, respectively (Fig. 1a). The two distinct plasmon absorption bands at 513 and 624 nm (Fig. 1B) corresponding to the transverse and longitudinal nanorod plasmon resonance are consistent with the past findings [15]. The functionalization of the GNRs by Folic Acid (FA) was obtained through the traditional EDC linkage. According to our previous report, GNRs were first modified by cystamine [14] and FA was activated by EDC [16] to complete this reaction. The modification of GNRs by FA and DOX was monitored by UV–Vis absorption spectra as shown in Fig. 2A. The longitudinal plasmon peak slightly red-shifted from 634 nm (a) to 640 nm (curve b) upon binding of FA onto the GNRs surface, confirming the FA functionalization protocol standardized in our previous works [13,17]. To quantitatively calculate the amount of DOX on the surface of GNRs, the UV–Vis absorption spectrum of DOX before and after interaction with GNRs was recorded (Fig. 2b). The typical absorption peak of DOX can be seen at approximately 488 nm. After interaction with GNRs, most of the free DOX was subjected to the UV–Vis as shown in curve b in Fig. 2B. We can also note the peak at about 630 nm, which is from the free GNRs in the DOX solution.

The concentration of DOX bound to GNRs can be calculated from the absorbance intensity of DOX using Beer's Law ($A = \varepsilon \times l \times c$, where '$A$' is the absorbance, '$l$' is the path length, '$c$' is the concentration and 'ε' is the absorption coefficient), which assumes that absorption is linearly proportional to concentration. From experiments, the concentration of DOX adsorbed onto GNRs was calculated to be 4.75 nM. For our calculations the absorption of known concentration of the original DOX obtained from UV–Vis analysis was used to calculate the absorption coefficient. This coefficient was then

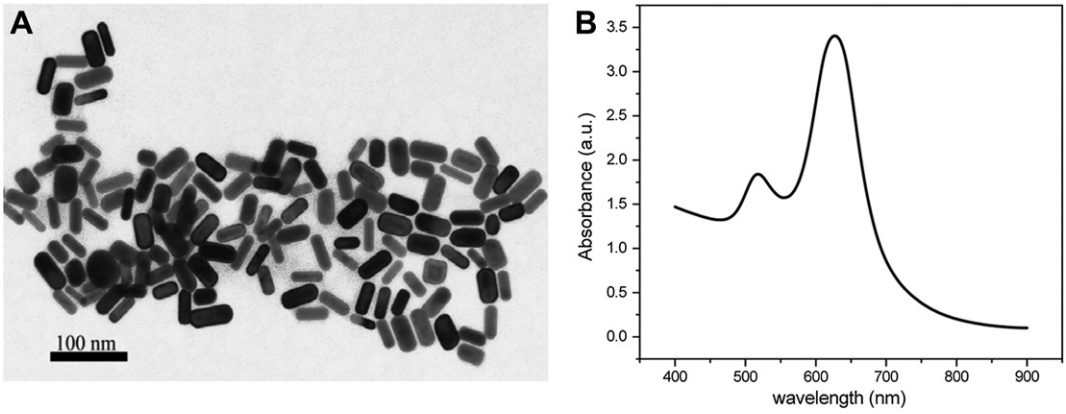

Fig. 1. TEM image (a) of GNRs and UV–vis absorption spectrum (b) of GNRs.

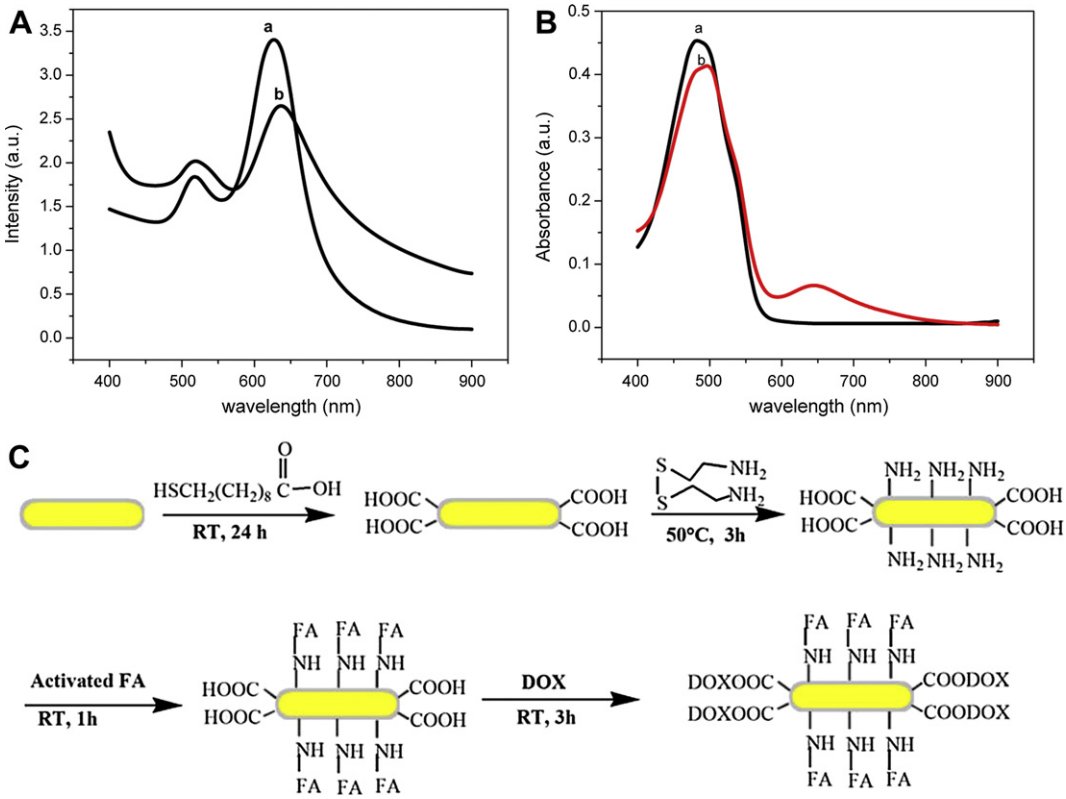

Fig. 2. (a) UV–Vis absorption spectra of GNRs (a) and GNRs bound with FA and DOX (b); (b) UV–vis absorption spectra of DOX before (a) and after bound with GNRs (b) (c) Schematic of GNR + FA + DOX formation process.

applied to Beer's law to calculate the concentration of DOX conjugated to GNRs. Previous literature has used a range of 0–10 nM for Doxorubicin dosing on the cell line and showed a dose-dependent growth inhibition [18]. Therefore, the dosage of 4.75 nM was within this range. This calculated concentration of DOX was also used for control experiments.

3.2. Cell preparation and imaging

KB cells were grown on 1 mm thick coverslips to approximately 80% confluency in RPMI 1640 growth media with 10% fetal bovine serum and penicillin/streptomycin and then incubated with the gold nanorod probes. Prior to each measurement, cells were washed three times with PBS and then imaged in PBS. Washing facilitated removal of unbound particles and removal of background from components of the media including phenol red. Each experiment consisted of four samples each, including multifunctional GNRs with FA and DOX, gold nanords with FA, DOX alone, and control cells which were grown under the same conditions, but not incubated with drugs or particles. All experiments were repeated at least four times. Doxorubicin was added at comparable concentrations and incubated with the GNRs. Uptake and fluorescence from the nanorods and DOX were measured in increments from 1 to 24 h. In these results, time intervals of 2 h, 4 h, and 16 h are represented. Representative images from each time point are depicted in the following figures. However for each slide 3 to 5 images were taken. Additional images from experiments for these time points as well as from 12 to 24 h are provided in the Supplementary information (Figs. S1–S7). An area of 80 × 80 μm was scanned in approximately 60 s with an excitation wavelength of 780 nm with a laser power of 32 mW from the 90 mHz pulsing two-photon laser. The images depict two-photon fluorescent lifetime and intensity.

3.3. Fluorescence lifetime fitting

Fluorescence lifetime measures the decay kinetics of a fluorophore as it transitions from excited state to ground state. The fluorescence lifetime of gold particles and DOX was determined from the time correlated single-photon counting (TCSPC) measurements (Fig. 3a and b). A 3-component exponential fit convolved with the instrument response function was used to fit the TCSPC curve. Each experiment was done in triplicate and the best fit calculated using chi-squared values. The fluorescent lifetime of GNRs was 0.34 ± 0.09 ns with an averaged chi-squared value of 8.06. The fluorescent lifetime of GNRs with covalently linked FA was 0.34 ± 0.07 ns with an averaged chi-squared value of 4.11. The TCSPC curve for GNRs alone was identical to that of GNRs conjugated with FA, because FA contains no innate fluorescence. Despite acquiring consist lifetimes in the 0.3 ns range, the lifetime of the gold nanorods is presumed to be below this value, since the limitation of the lifetime fitting is 0.3 ns which correlates with the instrument response function. Previous literature has stated that the lifetime of GNRs may have an upper limit of ~50 fs, from theoretical calculations, but the limitation of the system cannot allow for measurements below 0.3 ns [19]. Therefore, the actual lifetime of GNRs may be below this 0.3 ns value. The fluorescent lifetime of the GNRs with FA and DOX (GNRs + FA + DOX) was 1.52 ± 0.08 ns. However, this value is representative of the fluorescent lifetime of DOX [20] and not the true GNRs. Since DOX was bound electrostatically, a smaller portion of the drug could be found in the solution to contribute to this reading. Since DOX has

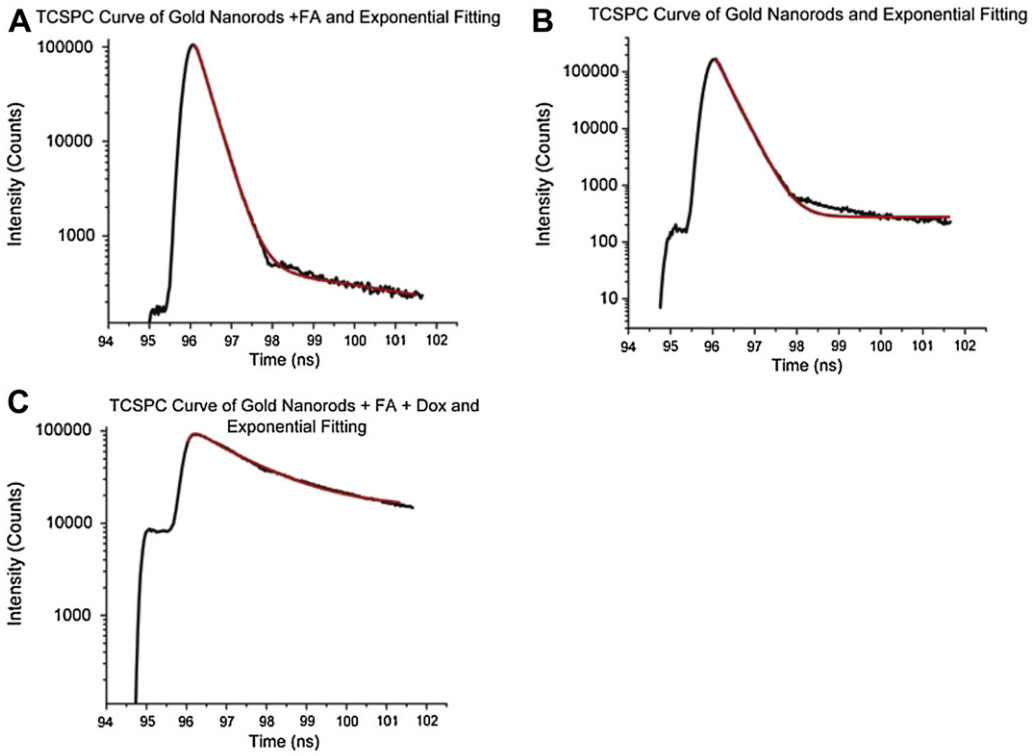

Fig. 3. Time correlated single-photon counting (TCSPC) measurements imaged with the multi-photon laser at an excitation wavelength of 780 nm and detected between 500 and 540 nm (a) depicts the TCSPC curve for the GNRs alone, (b) denotes GNRs + FA, and (c) shows the lifetime of DOX. Black lines represent raw data while the red lines are the convolved exponential fittings. (For interpretation of the references to colour in this figure legend, the reader is referred to the web version of this article.)

very high intensity; even a small amount of DOX in the solution can override the signal from GNRs.

3.4. Fluorescence lifetime imaging

Representative multi-photon confocal fluorescence lifetime images at critical time points are provided and discussed. Further images are provided in Supplementary Figs. S1–S7. Fig. 4 depicts the results after 2 h of incubation with the aforementioned samples. Fig. 4a shows the KB cells without addition of nanomaterials or drug additives. The image shows cellular autofluorescence from the membrane, cytoplasm, and various other cellular proteins. It should be noted that the intensity of the intensity scale in this image is ten times lower than the images of cells incubated with nanoparticles or drug (which exhibit intense fluorescence) as expected because the intensity of autofluorescence is much lower than that of the photoluminescent GNRs. The image of gold nanorods conjugated with FA alone is presented in Fig. 4b. Here we show the targeting of the nano-vehicles to folate receptor expressing KB cells. Blue color represents the lifetime of nanorods which is approximately 0.3 ns. In Fig. 4c we show the distribution of DOX in the cell. In this image, it can be noted that the drug has diffused inward and primarily resides in the cytoplasm of the cell. Fig. 4d, the image displays attachment of the GNRs coated with FA and DOX. Higher intensity areas can be seen on the membrane as well as a few spots in the interior of the cell depicting the release of DOX which has innate fluorescence. However, when it is in close proximity to the gold nanomaterial, its fluorescence is quenched. One can hypothesize that DOX is released from GNRs based on a difference in pH, which disrupts the electrostatic bonds. Decreased pH is due to localization inside transport vesicles constituting primarily the endosomes and lysosomes where the pH is approximately 5.0 [21]. This also is consistent with our previous work on localization of Herceptin coated gold nanorods [22]. Images of DOX alone after 1 h of incubation are provided in the Supplementary Fig. S1.

After 4 h of incubation with the aforementioned samples, the control as seen in Fig. 5a displayed consistent levels of fluorescence. Cells retain their autofluorescence and appear to be healthy in transmission images. The GNRs with FA alone show the same distribution as in the 2 h sample (Fig. 5b). However, the samples with DOX alone show drastic changes. The density of the cell population on the coverslip decreases to approximately 40% confluency visualized through a wide-field microscope. Images of the cells are as seen in Fig. 5c show DOX has permeated throughout the entirety of the cells including the nucleus, and the cells are undergoing rapid cell death. In Fig. 5d, a similar distribution of GNRs and DOX in the membrane and cytoplasmic regions can be noted. The fluorescent lifetime indicates that a percentage of DOX has been released, but the majority of the drug still remained in the quenched state due to its proximity to the nanorods.

After 16 h of incubation, vast changes were noted in the experimental samples incubated with drug loaded nanorods compared to the controls. The control cells which were not incubated with any drugs or nanoprobes appear healthy and exhibit a constant fluorescence (Fig. 6a). Cells incubated with GNRs functionalized with FA (GNRs + FA) remain healthy and the nanorods can still be detected via the difference in lifetime between autofluorescence and the nanorods (Fig. 6b). However, changes can be seen in Fig. 6c. There is an increase in the amount of fluorescence and its distribution throughout the cell. The lifetime of this fluorescence directly correlates to that of DOX. DOX is distributed throughout the cell and highly localized to the nuclear region as seen from its fluorescence. We expect the DOX to be detached from

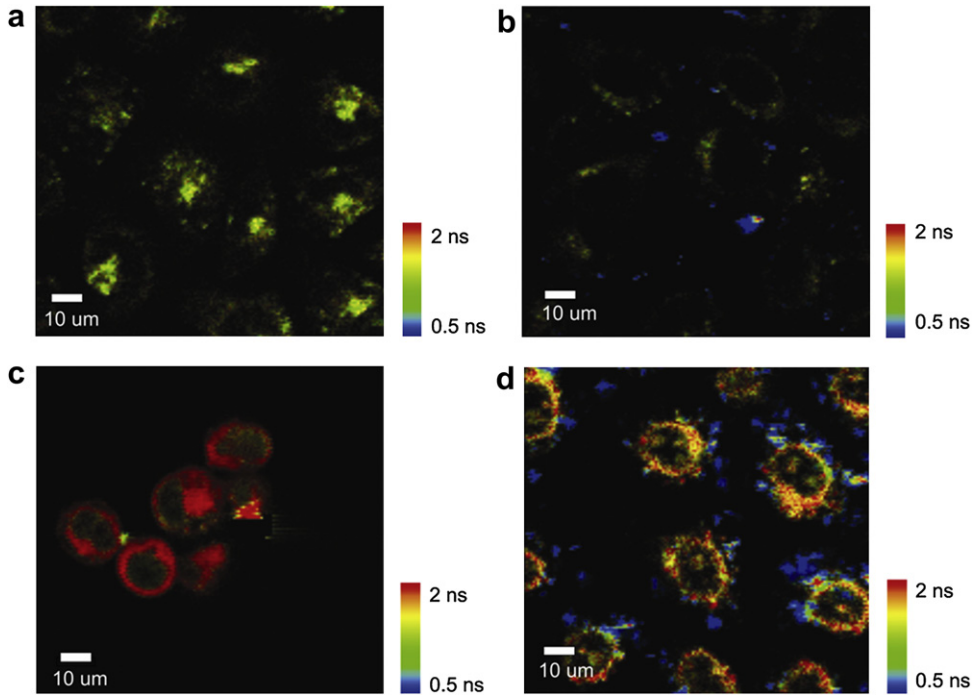

Fig. 4. Fluorescent lifetime confocal images of cells after 2 h of incubation (a) control KB cells alone (b) KB cells incubated with GNRs + FA (c) KB cells incubated with DOX alone (d) KB cells incubated with GNRs + FA + DOX the intensity values are constant in images 4b, 4c, and 4d with a range of 0–1000. In image 4a, the intensity is 0–100 in order to view the autofluorescence from the cell itself.

GNRs because its fluorescence is not quenched any longer. Cells were imaged again at 20 h and 24 h. At 20 h, the confluency decreased to approximately 15% due to cell death. At 20 h only a few groups of cells remained (Supplementary Fig. S6) and at 24 h, virtually no cells were available for imaging. To ensure that cell death was occurring and not mere detachment of the cells, Hoechst staining was utilized. Hoechst staining was completed in control KB cells incubated with PBS solution and in cells containing the gold

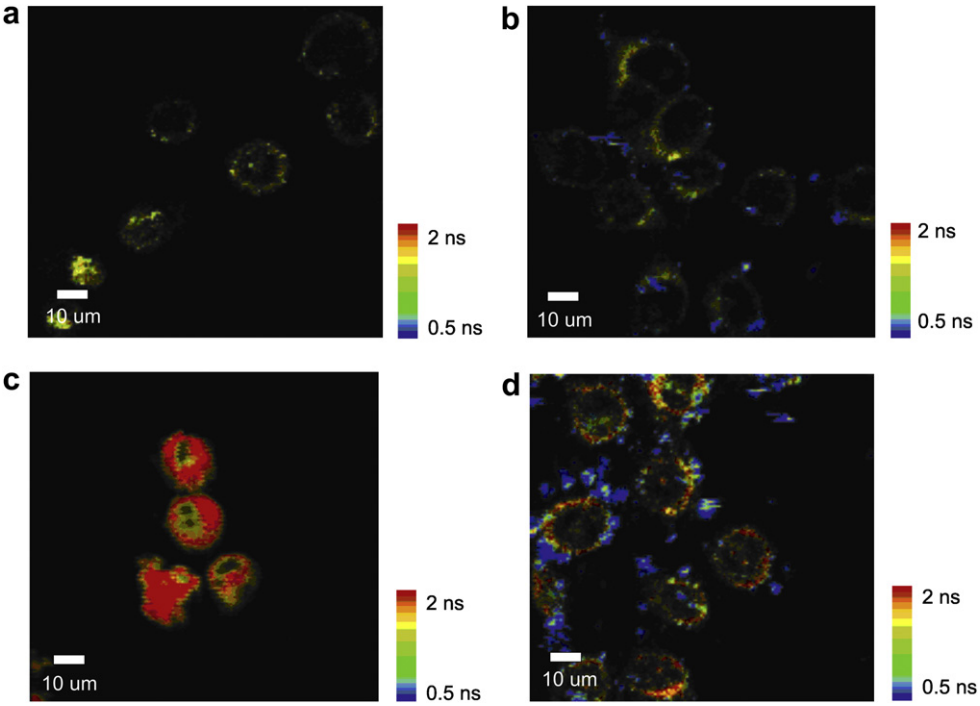

Fig. 5. Fluorescent lifetime confocal images of cells after 4 h of incubation (a) control-KB cells alone (b) KB cells incubated with GNRs + FA (c) KB cells incubated with DOX alone (d) KB cells incubated with GNRs + FA + DOX. The intensity values are constant in images 5b, 5c, and 5d with a range of 0–1000. In image 5a, the display intensity is set to a range of 0–100 for visualization because cellular autofluorescence is not as intense as the emission from DOX or GNRs.

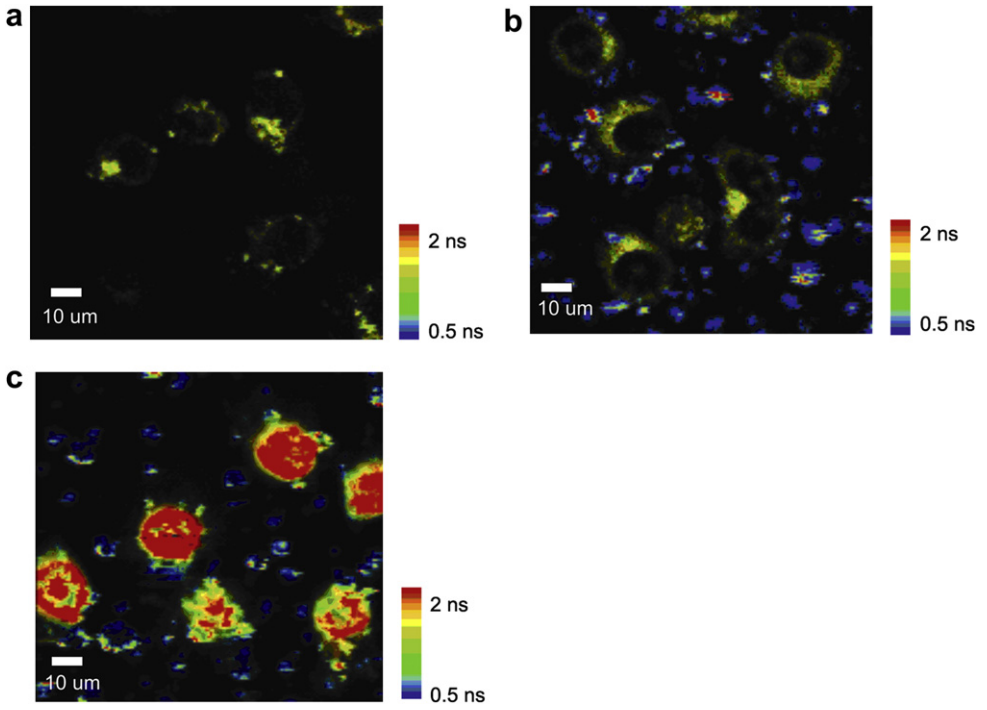

Fig. 6. Fluorescent lifetime confocal images of cells after 16 h of incubation (a) control-KB cells alone (b) KB cells incubated with GNRs + FA (c) KB cells incubated with GNRs + FA + DOX. The intensity values are constant in images 6c with a range of 0–1000. In image 6a, 6b, the intensity is scaled to 0 to 100 to visualize the less intense cellular autofluorescence. Cells incubated with DOX alone are not included in this image, because cell death occurred and cells could not be imaged after 4 h of incubation with the drug.

nanorods with FA and DOX. Results are provided in Supplementary Fig. S8. Samples depicted represent incubation with PBS for 24 h and with the nanorods sample for 8 h. The Hoechst stain labels DNA, our results show that for the duration of our experiments, cells in PBS depict a healthy nucleus with homogenously spread DNA. However, in the nanorod samples, the DNA is condensed into spherical vesicles demonstrating the cells are undergoing induced cell death.

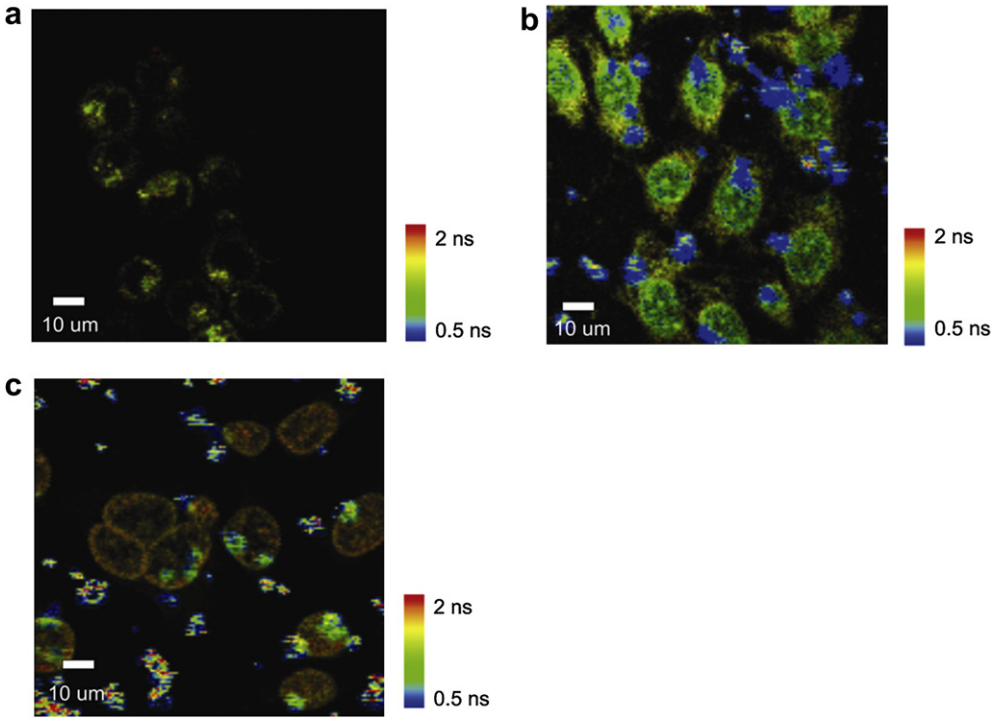

Fig. 7. Fluorescent lifetime confocal images of MDA-MB 468 cells after 24 h of incubation (a) control MDA-MB 468 cells alone (b) MDA-MB 468 cells incubated GNRs + FA (c) MDA-MB 468 cells incubated with GNRs + FA + DOX. The intensity values are constant in images with a range of 0–100.

3.5. Control experiments

Control experiments were conducted to show the specificity of the targeting ligand and were demonstrated by incubation of the targeting vehicle with MDA-MB 468 breast cancer cells, which do not over express folate receptors [23]. Control cells were incubated with the gold nanoparticles and imaged using the same excitation power and experimental conditions. To demonstrate the efficiency of targeting, cells were incubated with the targeted nano-vehicles for up to 24 h and then imaged using the same protocols as previously stated. Results can be seen in Fig. 7. Fig. 7a depicts the autofluorescence of the breast cancer cells and the intensity is the same as that of autofluorescence of the KB cells. Fig. 7b shows GNRs with FA incubated with the cells. A significantly lower percentage of binding occurred on the surface of these cells. Fig. 7c portrays the results of incubation with the GNRs functionalized with DOX and FA (GNRs + FA + DOX). A small amount of DOX, determined by its lifetime can be seen within the nucleus of the cells. However, this could be due to the release of DOX in solution, since DOX was bound to the particles electrostatically and may have a higher rate of dissociation. After time, a percentage of the drug is expected to be released and will then be free to diffuse directly into the cell. Comparison between the KB cells at 16 h and the MDA-MB 468 cells at 24 h shows a distinct difference in the amount and effect of DOX on these cell lines.

4. Conclusion

This work characterized the release and functioning of a currently used anti-cancer drug using two-photon fluorescence microscopy. It also created a successful and specific vector for targeted delivery of this drug to only cells over expressing a specific surface receptor. By fabricating multifunctional gold nanorods targeting the over expressed folic acid receptor, we show that cancer cells receive a significantly higher dosage of the drug than normal cells thereby minimizing the drug effect on normal cells while targeting and killing the cancer cells. This work provides evidence of a high level of targeting by demonstrating differences in uptake of cells with different levels of folate receptor expression.

Future applications of this work may include alterations of the target from folic acid to other known over expressed receptors such as Her2/Neu or EGFR. This targeting vehicle can be utilized for various methods of personalized medicine. Future directions for this work include application of this technique to tissue samples and live animal studies. Alternative work may also include application of this vehicle as a dual therapy agent via photothermal ablation as the dimensions of this particle are advantageous for this type of study. In conclusion, this research is one of the first of many significant strides in the progression of cancer targeting and personalized nanomedicine.

5. Experimental protocols

5.1. Preparation of GNRs

CTAB-stabilized GNRs were synthesized by the seed-mediated growth method improved by El-Sayed and Nikoobakht [24]. Briefly, the seed solution was prepared by mixing CTAB (0.2 M, 5 mL) and $HAuCl_4$ (0.5 mM, 5 mL) with freshly prepared ice-cold $NaBH_4$ (10 mM, 600 μL). The seed solution was then used for the synthesis of GNRs 3–5 h after preparation. CTAB (0.2 M, 20.0 mL) was mixed with silver nitrate (10 mM, 120 μL) and $HAuCl_4$ (1 mM, 20.0 mL) in two separate flasks and gently mixed and ascorbic acid (0.10 M, 240 μL) was added. To this mixture, the seed solution (48 μL) was finally added to initiate growth to yield GNRs with an aspect ratio of approximately 2.8. Excess CTAB was removed by centrifuging twice at 8000 rpm. The supernatant was discarded and the particles were redispersed in pure water.

5.2. Absorption measurements of GNRs

Absorption spectra of GNRs, GNRs-FA and the multifunctional GNRs-FA + DOX functionalized were measured with a Jasco V570 UV/Visible/NIR spectrophotometer (Jasco, Inc., Easton, MD) in the 400 and 900 nm wavelength ranges.

5.3. Cell culture

KB cells were grown in RPMI 1640 (Invitrogen) media without FA with 10% fetal bovine serum and penicillin streptomycin. Cells were grown as an adherent culture in 25 mL flasks and incubated at 37 °C with 5% carbon dioxide. Cells were split when they reached 70–80% confluency. For splitting, cells were first washed with Hank's balanced salt solution and incubated with 0.25% trypsin–EDTA for detachment from the flask. Then, trypsin–EDTA was diluted in the ratio 1:10 with media and cells were reconstituted in new flasks. Cells were grown up to 18 mm in diameter on 1 mm thick glass slides (VWR International, Batavia, IL) for imaging and 1 mL of cell media mixture was added to each well of a 6 well plate and replaced as necessary. The media was then replaced with phosphate buffered solution (PBS) for imaging as the media contained phenol red which could potentially interfere with imaging and contribute to autofluorescence.

5.4. Hoechst staining protocol (Supplementary Figs.)

Cell death was monitored by Hoechst staining (See Supplementary information for resulting images). Cells were fixed with 4% paraformaldehyde. They were washed three times in PBS for 5 min each. The cells were then permeabilized with 0.1% Triton X-100 for 10 min and subjected to washing with PBS three times. Then the cells were incubated with 2 μg/mL of Hoechst stain for 15 min. Cells were washed with PBS three times and then imaged by fluorescence microscopy.

5.5. Multi-photon imaging

A Coherent Chameleon XR pulsing laser which emitted at 780 nm (tunable range is from 750 to 980 nm) with an operating frequency of 90 MHz was used for imaging. A Picoquant Microtime 200 system was utilized to focus the laser beam through a 100× water immersion objective lens with a numerical aperture of 0.75. Light was collected through the same objective lens and its intensity was measured using an avalanche photo diode with an emission filter of 520/40. Intensity and lifetime images and values were measured throughout a 60 s raster scan of an 80 μm by 80 μm area.

Acknowledgements

This research was partly supported by a grant from the Purdue Center for Cancer Research and a grant from the Clinical and Translational Sciences Institute (Purdue-IUPUI) and the Indo-US Knowledge Network grant. The Ross Fellowship to Brittany Book from the College of Engineering is acknowledged.

Appendix. Supplementary information

Supplementary information associated with this article can be found, in the online version, at doi:10.1016/j.ejmech.2011.12.036.

References

[1] (a) A. Mooradian, Photoluminescence of metals, Phys. Rev. Lett. 22 (1969) 185–187;
(b) H. Wang, T.B. Huff, A.A. Wei, J.X. Cheng, In vitro and in vivo two-photon luminescence imaging of single gold nanorods, Proc. Natl. Acad. Sci. 102 (2005) 15752–15756.

[2] G.T. Boyd, Z.H. Yu, Y.R. Shen, Photoinduced luminescence from the noble metals and its enhancement on roughened surfaces, Phys. Rev. 33 (1986) 7923–7936.

[3] J. Turkevich, P.C. Stevenson, J. Hillier, The formation of colloidal gold, J. Phys. Chem. 57 (1953) 670–673.

[4] M. Brust, M. Walker, D. Bethell, D.J. Schiffrin, R.J. Whyman, Synthesis of thiol-derivatised gold nanoparticles in a two-phase liquid–liquid system, J. Chem. Soc. Chem. Commun. (1994) 801–802.

[5] S.D. Perrault, W.C.W. Chan, Synthesis and surface modification of highly monodispersed, spherical gold nanoparticles of 50–200 nm, J. Am. Chem. Soc. 131 (2009) 17042–17043.

[6] (a) S.D. Weitman, R.H. Lark, L.R. Coney, D.W. Fort, V. Frasca, V.R. Zurawski Jr., B.A. Kamen, Distribution of the folate receptor GP38 in normal and malignant cell lines and tissues, Cancer Res. 52 (1992) 3396–3401;
(b) I.G. Campbell, T.A. Jones, W.D. Foulkes, J. Trowsdale, Folate-binding protein is a marker for ovarian cancer, Cancer Res. 51 (1991) 5329–5338;
(c) M.S. Jhaveri, A.S. Rait, K. Chung, J.B. Trepel, E.H. Chang, Antisense oligonucleotides targeted to the human α folate receptor inhibit breast cancer cell growth and sensitize the cells to doxorubicin treatment, Mol. Cancer Ther. 3 (2004) 1505–1512.

[7] M. Fenech, C. Aitken, J. Rinaldi, Folate, vitamin B12, homocysteine status and DNA damage in young Australian adults, Carcinogenesis 19 (1998) 1163–1171.

[8] G.E. Kellog, J.N. Scarsdale, F.A. Fornari, Identifation and hydropathic characterization of structural features affecting sequence specificity for doxorubicin intercalation into DNA double-stranded polynucleotides, Nucleic Acids Res. 26 (1998) 4721–4732.

[9] R.L. Momparler, M. Karon, S.E. Siegel, F. Avila, Effect of adriamycin on DNA, RNA, and protein synthesis in cell-free systems and intact cells, Cancer Res. 36 (1976) 2891–2895.

[10] K.M. Tewey, T.C. Rowe, L. Yang, B.D. Halligan, L.F. Liu, Adriamycin-induced DNA damage mediated by mammalian DNA topoisomerase II, Science 226 (1984) 446–468.

[11] (a) E. Schneider, Y. Hsiang, L.F. Liu, DNA topoisomerases as anticancer drug targets, Adv. Pharmacol. 21 (1990) 149–183;
(b) M. Sander, T. Tsieh, Double strand DNA cleavage by type II DNA topoisomerase from *Drosophilia melanogaster*, J. Biol. Chem. 258 (1983) 8421–8428;
(c) N.F. Bachur, F. Yu, R. Johnson, R. Hickey, Y. Wu, L. Malkas, Helicase inhibition by anthracylcline anticancer agents, Mol. Pharmacol. 41 (1992) 993–998;
(d) J.W. George, S. Ghate, S.W. Matson, J.M. Bertsman, Inhibition of DNA helicase II unwinding and ATPase activities by DNA-interacting ligands, J. Biol. Chem. 267 (1992) 10683–10689.

[12] T.B. Huff, M.N. Hanse, Y. Zhao, J.X. Cheng, A. Wei, Controlling the cellular uptake of gold nanorods, Langmuir 23 (2007) 1596–1607.

[13] C. Yu, J. Irudayaraj, Multiplex biosensor using gold nanorods, Anal. Chem. 79 (2007) 572–579.

[14] C. Wang, J. Irudayaraj, Gold nanoprobes for the detection of multiple pathogens, Small 4 (2008) 2204–2208.

[15] C.J. Orendorff, L. Gearheart, N.R. Jana, C.J. Murphy, Aspect ratio dependence on surface enhanced Raman scattering using silver and gold nanosubstrates, Phys. Chem. Chem. Phys. 8 (2006) 165–170.

[16] H.S. Yoo, T.G. Park, Folate-receptor-targeted delivery of doxorubicin nano-aggregates stabilized by doxorubicin-PEG-folate conjugate, J. Control. Release 100 (2004) 247–256.

[17] (a) C.S. Yu, H. Nakshatri, J. Irudayaraj, Identity profiling of cell surface markers by multiplex gold nanorod probes, Nano Lett. 7 (2007) 2300–2306;
(b) C.X. Yu, J. Irudayaraj, Quantitative evaluation of sensitivity and selectivity of multiplex NanoSPR biosensor assays, Biophys. J. 93 (2007) 3684–3692.

[18] J. Baselga, L. Norton, H. Masui, A. Pandiella, K. Coplan, W. Miller, Antitumor effects of doxorubicin in combination with anti-epidermal growth factor receptor monoclonal antibodies, J. Natl. Cancer Inst. 85 (1993) 1327–1333.

[19] S. Eustis, N. El-Sayed, Aspect ratio dependence of the enhanced fluorescence intensity of gold nanorods: experimental and simulation study, J. Phys. Chem. B 109 (2005) 16350–16356.

[20] X. Dai, Z. Yue, M.E. Eccleston, J. Swartling, N.K.H. Slater, C.F. Kaminski, Fluorescence intensity and lifetime imaging of free and micellar-encapsulated doxorubicin in living cells, Nanomedicine 4 (2008) 49–56.

[21] R. Lee, S. Wang, P.S. Low, Measurement of endosome pH following folate receptor-mediated endocytosis, Biochim. Biophys. Acta 1312 (1996) 237–242.

[22] J. Chen, J. Irudayaraj, Quantitative investigation of compartmentalized dynamics of ErbB2 targeting gold nanorods in live cells by single molecule spectroscopy, ACS Nano 3 (2009) 4071–4079.

[23] R. Meier, T.D. Henning, S. Boddington, S. Tavri, S. Arora, G. Piontek, M. Rudelius, C. Corot, H.E. Daldrup-Link, Breast cancers: MR imaging of folate-receptor expression with the folate-specific nanoparticle P1133, Radiology 255 (2010) 527–535.

[24] B. Nikoobakht, M.A. El-Sayed, Preparation and growth mechanisms of gold nanorods (NRs) using seed mediated growth method, Chem. Mater. 15 (2003) 1957–1962.